Nucl. Fusion **48** (2008) 084004 (6pp) doi:10.1088/0029-5515/48/8/084004

MHD induced neutral beam ion loss from NSTX plasmas

D.S. Darrow[1], **E.D. Fredrickson**[1], **N.N. Gorelenkov**[1], **A.L. Roquemore**[1] **and K. Shinohara**[2]

[1] Princeton Plasma Physics Laboratory, PO Box 451, Princeton, NJ 08543-0451, USA
[2] Japan Atomic Energy Agency, Naka, Ibaraki, Japan

Received 11 December 2007, accepted for publication 20 March 2008
Published 26 June 2008
Online at stacks.iop.org/NF/48/084004

Abstract
Bursts of ~60 kHz activity on Mirnov coils, identified as energetic particle modes, occur frequently in NSTX plasmas and these are accompanied by bursts of neutral beam ion loss over a range in pitch angles. These losses have been measured with a scintillator type loss probe imaged with a high speed (>10 000 frames s^{-1}) video camera, giving the evolution of the energy and pitch angle distributions of the lost neutral beam ions over the course of the events. The instability occurs below the TAE frequency in NSTX (~100 kHz) in high beta plasmas and may also be identified as a beta-induced Alfvén acoustic (BAAE) mode.

The data from one burst that causes a 13% reduction in the neutron rate have been studied extensively and have several interesting features. First, the burst begins with the mode having a purely $n = 1$ character, sweeping downwards in frequency. However, there is no change to the underlying loss signal during this time interval. This indicates there is no phase space transport of fast (80 keV D) ions into the loss cone seen by the probe from the frequency sweeping. As the burst evolves further in time, a concurrent $n = 2$ mode arises, followed quickly by a concurrent $n = 3$ mode. During this period when multiple modes are present, loss over a wide range of pitch angles is seen simultaneously, suggesting stochastization of the beam ion phase space. There is no evidence of any sweeping in pitch angle of the loss in either phase of the burst, at least not on the 100 μs time scale.

PACS numbers: 52.25Xz, 52.35Py, 52.55.Fa

1. Introduction

Magnetohydrodynamic (MHD) instabilities in magnetically confined plasmas can often be driven by a population of superthermal ions. In addition, such, instabilities can often cause the loss of energetic ions from the plasma. The National Spherical Torus Experiment (NSTX) [1] is a low aspect ratio tokamak heated by up to 8 MW of 90 kV deuterium neutral beams. Here, we describe observations of a bursting MHD mode driven by energetic neutral beam heating ions and which is detected by a Mirnov coil outside the plasma and which produces loss of those fast ions to a detector located at the vacuum vessel wall. The modes may fall in the category of energetic particle modes (EPMs) [2, 3]. The fast ion loss detector in NSTX [4] is of a scintillator type, which measures the pitch angle and gyroradius of the lost ions as a function of time. The probe acts as a magnetic spectrometer, using a pair of apertures and the confining magnetic field of the plasma to disperse lost fast ions onto a scintillator plate where their strike

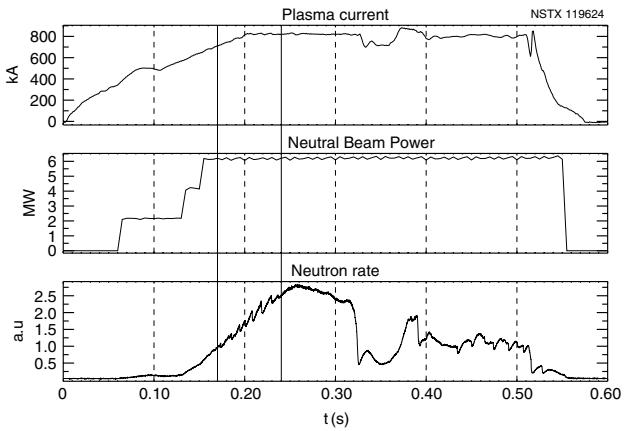

Figure 1. Plasma current in (kA) in the top panel, neutral beam power (MW) in the middle panel and neutron rate (a.u.) in the bottom panel for NSTX pulse number 119624. During the interval outlined by the two solid vertical lines, there are repeated drops in the neutron rate that are attributable to EPMs.

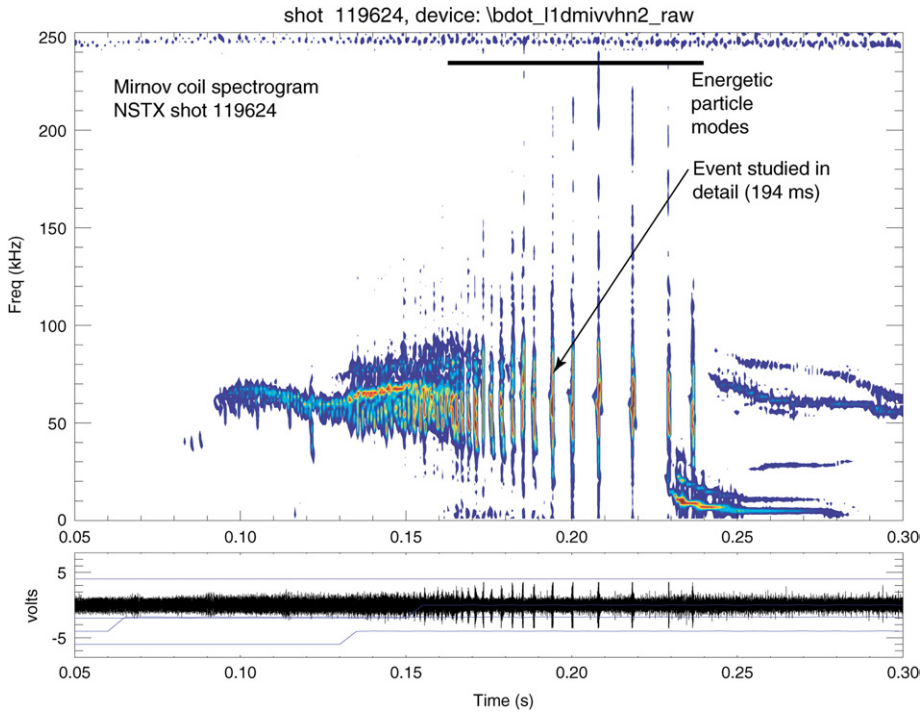

Figure 2. The upper panel shows the frequency spectrogram of magnetic fluctuations versus time in pulse 119624. Note the repeated short EPM bursts occurring during the interval marked by the bar near the top of the plot. The lower panel shows the raw Mirnov coil voltage versus time. In this paper, detailed analysis is made of the event marked by the arrow, at 194 ms.

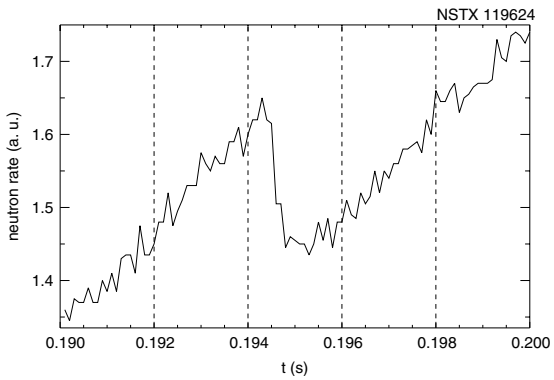

Figure 3. Neutron rate versus time over the course of the burst under study. The total neutron rate drops by 13% as a result of the single burst, with the drop in rate beginning at ∼194.3 ms.

point is determined by their pitch angle and gyroradius. For this experiment, the luminosity pattern on the scintillator plate was imaged by a fast framing rate intensified video camera (Photron Fastcam operated at 13 500 frames s^{-1}) in order to obtain high time resolution of the parameters of the lost ions.

2. Results

Figure 1 displays the time evolution of the plasma current, neutral beam heating power, and neutron rate of NSTX pulse 119624. In the portion of the pulse between the solid vertical lines in this figure, numerous rapid drops in the neutron rate are observed. These drops in the neutron rate coincide with brief bursts of MHD activity detected by a Mirnov coil in the vacuum vessel. The frequency spectrogram of these bursts is shown in figure 2. Such bursts occur commonly and repeatedly in NSTX discharges over a wide range of parameters. We choose to focus on the burst at 194 ms as a typical case. Figure 3 shows the evolution of the neutron rate before, during, and after this burst, which results in ∼13% drop in the neutron rate, indicative of the loss of a significant fraction of the neutral beam ions in the plasma, as neutron production in NSTX is essentially all due to beam–plasma reactions and the plasma density profile does not change appreciably during these events. Note that the drop in neutron rate commences at about 194.3 ms.

Figure 4 shows the frequency spectrogram of the burst on an expanded time scale. The burst can be divided into two intervals in time. It starts as an $n = 1$ mode at 65 kHz, which chirps downwards in frequency to 40 kHz in the course of 0.5 ms. Towards the end of the frequency chirp, an $n = 2$ mode arises and, shortly thereafter, an $n = 3$ mode also develops. In this phase of the burst, at least two modes of different n numbers are present concurrently until the burst ends. Figure 5 shows the spectrum of the Alfvén continuum for this time in the discharge, as calculated by the ideal MHD code NOVA-K [5] using the experimentally measured magnetic equilibrium and plasma profiles. NOVA-K is a perturbative code and it is therefore not able to calculate the characteristics of EPMs in this discharge. We argue that the observed modes fall within the wider EPM class because the beam ion beta is typically comparable to the plasma beta and the mode frequencies seem to be substantially below the TAE frequency. Here, NOVA-K is used simply to determine the mode frequencies and eigenmode structures within the ideal MHD approximation. The code is applied to the highest observed toroidal mode number, $n = 3$, in order to improve the numerical convergence of the solutions

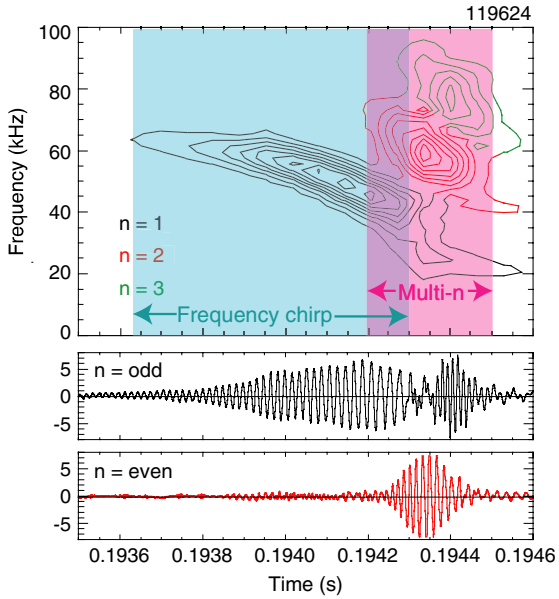

Figure 4. Expanded frequency spectrogram of the burst under study. The upper panel shows contours of mode amplitude versus frequency and time. The burst commences as a mode with a toroidal mode number $n = 1$ which chirps downwards in frequency. This is shown in the black amplitude contours, and the period of frequency chirping is outlined in pale blue. Subsequently, the mode spawns an $n = 2$ mode, shown in the red contours, that exists concurrently with the $n = 1$ mode. Shortly thereafter, an $n = 3$ mode also arises, shown in the green contours. During this interval, outlined by the lavender box and labelled 'multi-n,' at least two different n number modes exist concurrently. The middle panel shows the Mirnov coil signal, filtered to retain only the signal coming from the odd n number modes. The bottom panel shows the Mirnov coil signal, but filtered to retain only the signal attributable to even n number modes.

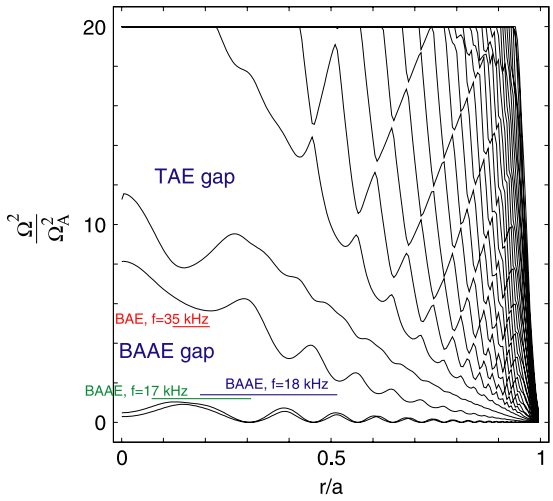

Figure 5. The Alfvén and acoustic gap diagram for this plasma at the time of the burst. This calculation shows a clear beta-induced Alfvén acoustic eigenmode (BAAE) gap for $n = 3$ at 18 kHz. The plasma rotation frequency at this time in the discharge is 20 kHz, giving a predicted mode frequency in the lab frame of 78 kHz for the $n = 3$ mode. This is identical to the observed frequency of the $n = 3$ mode in the burst, as shown in figure 4.

since higher n modes in general are more radially localized and thus interact less with the continuum. From NOVA-K, it is found that the $n = 3$ mode seen in figure 4 lies in the middle of the beta-induced Alfvén acoustic eigenmode (BAAE) [6] gap marked in the figure. This mode appears at 18 kHz in the plasma rest frame. At this time in the discharge, charge exchange spectroscopy indicates that a significant portion of the central region of the plasma is rotating with a frequency of 20 kHz, giving a predicted mode frequency in the lab frame of 78 kHz. Here we use the expression $f_{\rm lab} = f_{\rm plasma} + nf_{\rm rot}$. This is identical to the observed frequency shown in figure 4, meaning that this mode is quite possibly a BAAE. Note that the potentially strong drive from fast ions can affect the BAAE frequency and structure. The identification of the $n = 1$ and $n = 2$ modes in this burst as BAAEs would also be consistent if their radial position is near that of the $n = 3$ mode indicated by the NOVA-K simulation. BAAEs at these several n numbers would all have essentially the same frequency in the plasma frame as they would lie in the same gap. The observed frequencies of the $n = 1$ and $n = 2$ modes would also be consistent with the modes being BAAEs, based on the above formula. Unfortunately, no measurements of the internal structure of the modes were available for this plasma. Shown also in figure 5 are two modes close in frequency, namely, a 17 kHz BAAE localized closer to the core and a 35 kHz beta-induced Alfvén eigenmode (BAE) [7], which are also candidate identifications of this mode, given the uncertainties in the rotation velocity and the mode location.

Figure 6 shows images from the fast ion loss probe during the initial phase of the burst. In this and the succeeding figure, the starting times of each frame, as reported by the camera's internal clock, are shown. These times are found to be synchronized with the NSTX digitizer times to within half a camera frame duration (36 μs). Before and during the frequency chirping portion of the burst, the loss images look identical to image A. This image shows a single luminous spot consistent with loss at a single pitch angle and gyroradius. This spot first appears when neutral beam source C (which is the most perpendicular of the three beam sources on NSTX and which has a tangency radius of 50 cm) starts injecting and it is interpreted as prompt orbit loss from that beam. This spot is steady in position, size and luminosity before the burst begins and through the frequency chirping phase of the burst as well. Indeed, it appears that this spot is constant before, during, and after the burst, which would be consistent with prompt loss behaviour during steady beam injection. In the later phases of the burst, there is loss evident at other positions on the scintillator, but those losses appear additive to this underlying prompt loss. Images B and C in figure 6 show the loss probe images as the burst enters the mode overlap or multi-n phase. Here, there total luminosity is greater. Note that the onset of the broad range of pitch angle loss in frame B of figure 6, taken at 194.296 ms, coincides with the time at which the total neutron rate begins its precipitous drop. The position of the luminosity in the scintillator plate in the images in figure 6 is consistent with loss of D beam ions at the primary injection energy of 90 kV, but lost over a wide range in pitch angles, in contrast to the single pitch angle of loss in frame A. (See figure 8 for the interpretation grid of pitch angle and gyroradius.) This transient loss of a wide range of pitch angles is similar to beam ion loss features seen in Alfvénic modes in the CHS device [8].

Figure 7 displays the loss probe images in the later part of

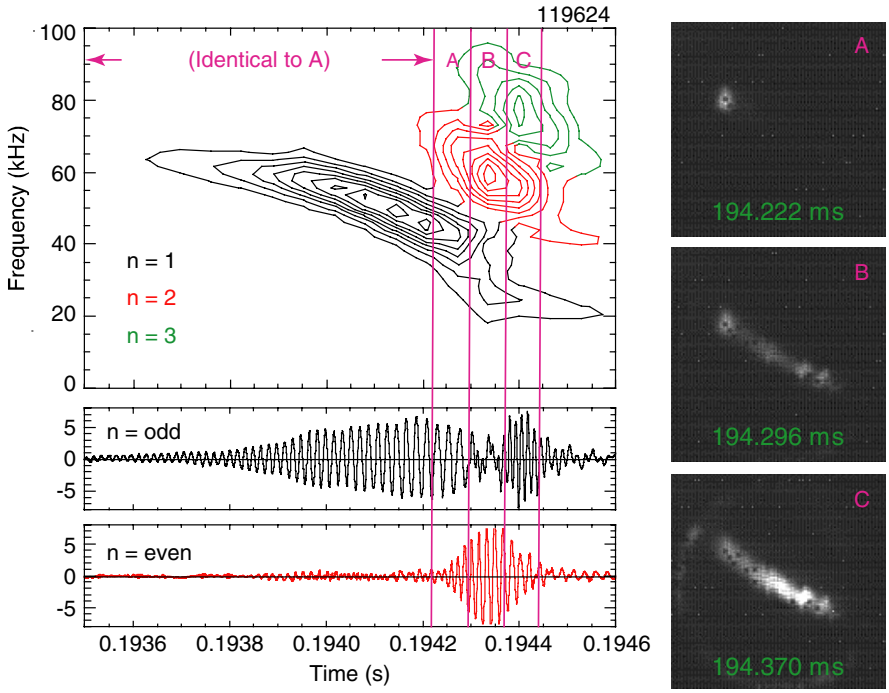

Figure 6. The left panel shows the frequency spectrogram of the burst again, with frame intervals of the fast ion loss probe demarcated by purple vertical lines and labelled by letter. The corresponding fast ion loss distribution images at each time interval are shown in the column at the right, along with the start time of each frame. In the fast ion loss probe images, more parallel-going particles appear at the left side of the frame, and more perpendicular moving particles appear toward the right side of the frame. Particle energy increases going from the lower left to the upper right of each image. A quantitative statement of the pitch angle and gyroradius of the losses is in figure 8. Note that the camera frames during the interval of frequency sweeping, before frame A, all appear identical in shape, position, and intensity to frame A, meaning that the frequency sweeping $n = 1$ mode does not cause particles to be lost to a position in phase space where they can be detected by the probe. Starting with frame B, there is loss over a broad range of pitch angles, coincident with the temporal overlap of two or more modes.

the burst as the concurrent modes decay. During this interval, the beam C prompt loss persists, but the wide pitch angle loss dims and then vanishes. The wide pitch angle loss vanishes as the mode overlap ends, suggesting strongly that it is this overlap which is responsible for the wide range of pitch angles lost. Frame E, taken starting at 194.519 ms, evidences the last significant traces of the broad range of lost pitch angles, and the total luminosity in this frame is clearly less than in frames B, C or D. This time correlates well with the time in figure 3 at which the neutron rate ceases to fall and reverts to its pre-burst rate of increase.

Figure 8 shows loss image B, taken when the multiple n number modes begin to overlap, with a superimposed grid to allow determination of the pitch angle and gyroradius of the lost ions. The image shows a loss at a gyroradius centroid of 25 cm which is reasonably consistent with the gyroradius of 20 cm expected for D beam ion loss at the full injection energy of 90 kV, given the magnetic field strength at the probe location. The modest discrepancy between the observed and expected gyroradius centroid value is believed to be due to a calibration error and not any actual acceleration of the lost particles and the lost ions extend over a range in pitch angle from 15° to 63°, i.e. from fairly parallel going to fairly perpendicular moving. Here, pitch angle is defined as $c = \arccos(v_{||}/v)$, where $v_{||}$ is the component of the particle's velocity that is along the local magnetic field at the probe.

3. Interpretation

The scintillator loss probe images do not show any significant change in the beam ion loss rate or characteristics before or during the frequency chirping phase of this burst. From theoretical considerations, one might expect that a frequency chirping mode could alter the energy or canonical angular momentum of fast ions, or both. A change in canonical angular momentum could result in radial transport of the affected particle. Certainly, no change in energy of the lost ions is seen during the chirping phase of the burst. Given that no change in the loss characteristics is seen during the chirping phase of a single mode, we conclude that either the frequency chirp is not causing radial transport of the fast ions, or is at least not causing transport into the loss cone at a point where the fast ion loss probe can detect it. This result is similar to that observed during the abrupt large amplitude events (ALEs) seen in JT-60U [9–11]. Modelling of ALEs, which have been identified as EPMs, showed significant internal redistribution of the fast ions during frequency chirping [12]. Secondly, we note that losses which are driven by the burst arise only at times when there are concurrent multiple n number modes present, e.g. during frames B, C, D and E in figures 6 and 7. These losses are at the primary beam injection energy and cover a wide range in pitch angle, as seen in figure 8. This loss during mode overlap is also seen to turn on and off quite quickly as the multiple n mode overlap starts and ends. The start and end times of the broad pitch angle loss coincide with the interval over which

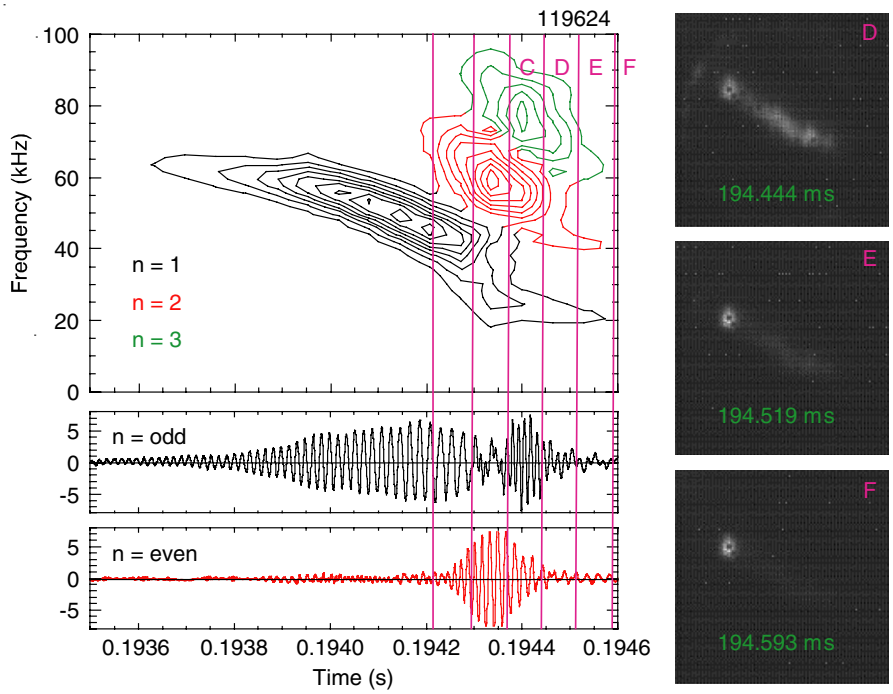

Figure 7. The spectrogram of the burst again, with fast ion loss probe frame intervals later than those in figure 6 demarcated. The corresponding fast ion loss distribution images at each time interval are shown in the column at the right, along with the start time of each frame. In frames D, E and faintly in F are seen a loss that extends over a wide range of pitch angles, similar to frames B and C in figure 6. These also occur during an interval when two different n number modes are present. In frame F, the loss has nearly returned to its pre-burst pitch angle, gyroradius, and intensity.

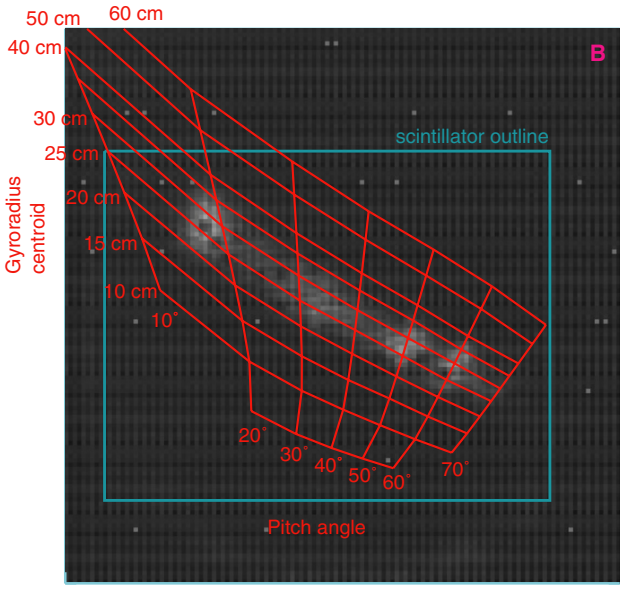

Figure 8. Loss image B from figure 6 with superimposed grid of pitch angle and gyroradius centroids. The loss appears at essentially a single gyroradius (25 cm) reasonably commensurate with the gyroradius of 20 cm expected for the 90 keV deuterons being injected. This modest discrepancy between predicted and measured gyroradius is believed to be due to calibration errors in the instrument and not due to any actual acceleration of the particles by the mode. The loss covers a range in pitch angle from 15° to 63°, and the interpretation of the range of pitch angles affected would be altered in only a minor way by the calibration error noted above.

the neutron rate is dropping. Furthermore, the fast ion loss during the concurrent multiple n mode phase of the burst does not show any evidence of sweeping or moving in pitch angle, at least not on a time scale that could be imaged by the camera used (73 μs/frame). This sweeping in pitch angle is something that might be expected to occur if resonance between modes and particles were causing the wide range of lost pitch angles seen. From these features, we believe that the wide pitch angle range lost arises from a stochastization of the fast ion phase space induced by the presence of multiple n number modes (i.e. modes of differing helicities or spatial structures). We do note, however, that locally stronger features of the loss, such as the two brighter spots toward the lower right of image B in figure 6 may arise from resonant mode–particle interactions.

Acknowledgments

This work was performed under US DoE contract DE-AC02-76-CH03073 and was supported by the Japanese Society for the Promotion of Science, Grant-in-Aid for Scientific Research (Encouragement of Young Scientists (B) No 16760681). We are indebted to the referees of this paper for the contribution of several relevant references.

References

[1] Spitzer J. *et al* 1996 *Fusion Technol.* **30** 1337
[2] Chen L. 1994 *Phys. Plasmas* **1** 1519
[3] Cheng C.Z., Gorelenkov N.N. and Hsu C.T. 1995 *Nucl. Fusion* **35** 1639
[4] Darrow D.S. 2008 *Rev. Sci. Instrum.* **79** 023502

[5] Cheng C.Z. and Chance M.S. 1986 *Phys. Fluids* **29** 3695
[6] Gorelenkov N.N., Berk H.L., Fredrickson E and Sharapov S.E. 2007 *Phys. Lett.* A **370/1** 70
[7] Turnbull A.D. *et al* 1995 *Phys. Fluids* B **5** 2546
[8] Shinohara K., Isobe M., Darrow D.S., Shimizu A., Nagaoka K. and Okamura S. 2007 *Plasma Fusion Res.* **2** 042
[9] Shinohara K. *et al* 2001 *Nucl. Fusion* **41** 603
[10] Shinohara K. *et al* 2002 *Nucl. Fusion* **42** 942
[11] Shinohara K. *et al* 2004 *Plasma Phys. Control. Fusion* **46** S31
[12] Briguglio S. *et al* 2007 *Phys. Plasmas* **14** 055905